Dispersion, Nonlinearity, and Viscosity in Shallow-Water Waves

By Steve Elgar,[1] R. T. Guza,[2] and M. H. Freilich[3]

Abstract: The roles of frequency dispersion, nonlinearity, and laminar viscosity in the evolution of long waves over distances of many wavelengths in constant water depth are investigated with numerical solutions of the Boussinesq equations. Pronounced frequency doubling and trebling is predicted, and the initial evolution to a wave shape with a pitched-forward front face and peaky crests is followed by development of a steep rear face and a nearly symmetric crest/trough profile. While reducing overall energy levels, laminar viscosity acts to prolong cycling of third moments and to inhibit the onset of disordered evolution characteristic of nonlinear, inviscid systems. Preliminary laboratory results show some qualitative similarities to the numerical simulations. However, these laboratory experiments were not suitable for detailed model-data comparisons because dissipation in the flume could not be accounted for with either laminar or quadratic damping models. More carefully controlled experiments are required to assess the importance of viscosity (and the accuracy of the Boussinesq model) in the evolution of nonlinear waves over distances of many wavelengths.

Introduction

The Boussinesq equations have been used successfully to predict observations of the evolution of inviscid, weakly nonlinear, weakly dispersive, unbroken gravity waves propagating on sloping beaches, both in the field (e.g. Freilich and Guza 1984; Elgar et al. 1990b) and the laboratory (e.g. Abbott et al. 1978; Madsen and Warren 1984; Liu et al. 1985; Vengayil and Kirby 1986). On plane beaches, both the models and the observations show nearly monotonic shoaling transformations, with initially symmetric, near-Gaussian waves becoming asymmetric and non-Gaussian prior to breaking. However, on even mildly sloping beaches, the shoaling region is typically less than about 5 wavelengths wide.

Longer evolution distances are, of course, possible in constant depth, and it is of interest to determine whether the monotonic shoaling transformations observed and modeled on sloping topography are generic features of long waves governed by the Boussinesq equations, or are the result of the decreasing depth in the direction of wave propagation. Furthermore, previous comparisons of Boussinesq model predictions with field data have not included dissipation. Although dissipation is not expected to have major effects over short distances characteristic of natural shoaling regions (and of many laboratory experiments), it may significantly alter the nonlinear evolution of the waves over longer distances.

For initial conditions of a single plane wave with frequency f_p, two-mode solutions of the Boussinesq equations—the only allowed motions are at

[1]Assoc. Prof. Elect. and Comp. Engrg., Washington State Univ., Pullman, WA 99164-2752.

[2]Prof., Ctr. for Coastal Studies, Scripps Inst. of Oceanography 0209, La Jolla, CA 92093.

[3]Assoc. Prof., College of Oceanic and Atmospheric Sciences, Oregon State University, Corvallis, OR 97331-5503.

Note. Discussion open until December 1, 1993. To extend the closing date one month, a written request must be filed with the ASCE Manager of Journals. The manuscript for this paper was submitted for review and possible publication on February 25, 1991. This paper is part of the ***Journal of Waterway, Port, Coastal, and Ocean Engineering***, Vol. 119, No. 4, July/August, 1993. ©ASCE, ISSN 0733-950X/93/0004-0351/$1.00 + $.15 per page. Paper No. 1427.

frequencies f_p and $2f_p$ (e.g. Mei and Ünlüata 1972)—predict perfect spatial recurrence in the absence of dissipation. However, when many modes are allowed (keeping the initial energy confined to f_p), the Boussinesq equations predict transfers of energy from the primary wave, first to its harmonics (frequencies $2f_p$, $3f_p$, . . .), but eventually also to nonharmonic frequencies, with damped recurrence cycles followed by disordered evolution of the Fourier modes (Elgar et al. 1990a). Numerical simulations, presented later, of wave fields composed initially of a sinusoid within a low-level background demonstrate that laminar viscosity increases the number of recurrence cycles relative to inviscid cases.

Both few- and many-mode inviscid models predict unusual wave shapes during various stages of evolution in constant depth. The initial evolution to a pitched-forward front face and peaky crests (usually a precursor to breaking on a sloping beach) is followed by development of a steep rear face and a nearly symmetric crest/trough profile. The present study also examines the effect of viscosity on these predictions.

There are few laboratory observations of the evolution of nonlinear long waves over long [$O(20)$ wavelength] distances. Mei and Ünlüata (1972) showed that Goda's appearance distances, the distance between successive maxima of energy at frequency $2f_p$, were in agreement with theory for the recurrence length of a two-mode system. However, owing to their short laboratory tank, Mei and Ünlüata could observe only a few recurrence cycles and did not report details of the observed wave profiles. Other laboratory studies (e.g. Buhr-Hansen and Svendsen 1974) span $O(20)$ wavelengths, but nonlinearity was very weak and cross-spectral energy transfers were correspondingly small. An additional purpose of the present study that was only marginally successful was to compare predictions of the viscous Boussinesq model with new laboratory observations spanning many wavelengths.

Boussinesq Model Results

The Boussinesq equations (Peregrine 1967, 1972) for unidirectional waves in a constant depth fluid are satisfied by a water surface η given by

$$\eta = \sum_{n=1}^{N} a_n(x)\cos[k_n x + \Phi_n(x) - \omega_n t] \quad \ldots\ldots\ldots\ldots\ldots\ldots\ldots\ldots\ldots\ldots (1)$$

where a_n and Φ_n = Fourier amplitudes and phases of the wave field, respectively; k_n = wave number at radian frequency ω_n (where $\omega_n = n\Delta\omega$ with $\Delta\omega$ the frequency resolution); and N = number of modes used to represent the wave field.

Substituting the expression for η into the Boussinesq equations and including the effects of laminar viscosity yields differential equations describing the spatial evolution of the modal amplitudes and phases, given schematically by

$$\dot{a}_n = \mathrm{NL} - a_n D_n \quad \ldots\ldots\ldots\ldots\ldots\ldots\ldots\ldots\ldots\ldots\ldots\ldots\ldots\ldots\ldots\ldots (2a)$$

$$\dot{\Phi}_n = \mathrm{NL} + D_n \quad \ldots\ldots\ldots\ldots\ldots\ldots\ldots\ldots\ldots\ldots\ldots\ldots\ldots\ldots\ldots\ldots (2b)$$

where the overdot indicates differentiation with respect to the propagation direction x; and NL = nonlinear terms (Freilich and Guza 1984). The viscous term D_n based on laminar boundary layers, both at the bottom and at the clean free surface is

$$D_n = \sqrt{\frac{\nu}{8\omega_n}}\frac{k_n}{h}\left[1 + \frac{5}{3}\left(\frac{\omega_n^2 h}{g}\right)\right] \quad \ldots\ldots\ldots\ldots\ldots\ldots\ldots\ldots\ldots\ldots\ldots\ldots (3)$$

where ν = kinematic viscosity; h = water depth; and g = gravity (e.g. Van Dorn 1966; Vengayil and Kirby 1986). The inviscid, small amplitude (linear) wave number k_n is given by

$$k_n = \frac{\omega_n}{(gh)^{1/2}}\left(1 + \frac{h\omega_n^2}{6g}\right) \quad \ldots\ldots\ldots\ldots\ldots\ldots\ldots\ldots\ldots\ldots\ldots\ldots\ldots\ldots (4)$$

Sidewall damping is negligible in the present case of a flume much wider than the depth (Van Dorn 1966).

The evolution equations (2) are strictly applicable to a deterministic system composed of motions at a finite set of fixed, discrete frequencies. Given a set of initial amplitudes and phases, (2) can be integrated numerically, as discussed in Freilich and Guza (1984) and Elgar et al. (1990a). Previous work comparing model predictions with field observations simulated the random sea surface by averaging results from many similar model integra-

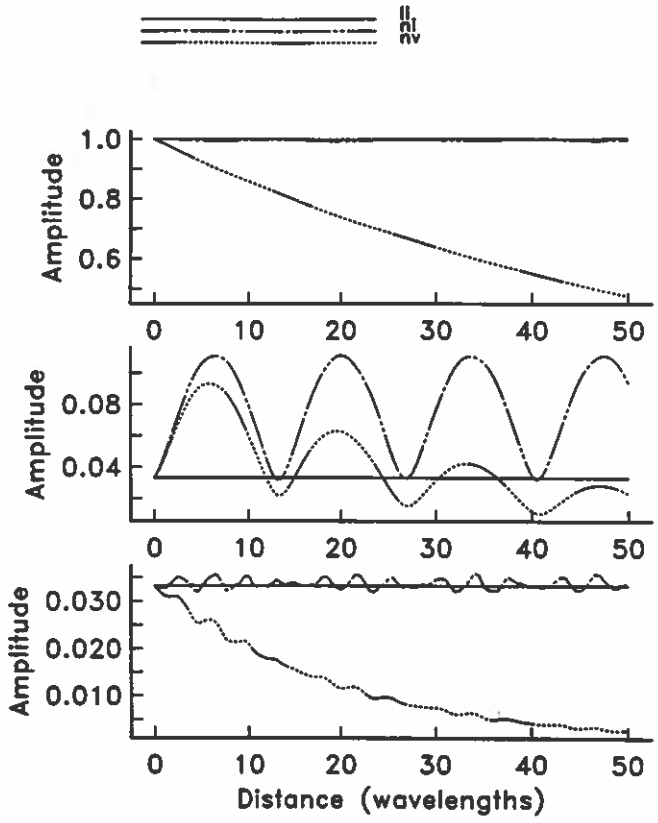

FIG. 1. Comparison of Evolution of Harmonic Amplitudes between Linear Inviscid (li), Nonlinear Inviscid (ni), and Nonlinear Viscous (nv) Boussinesq Models

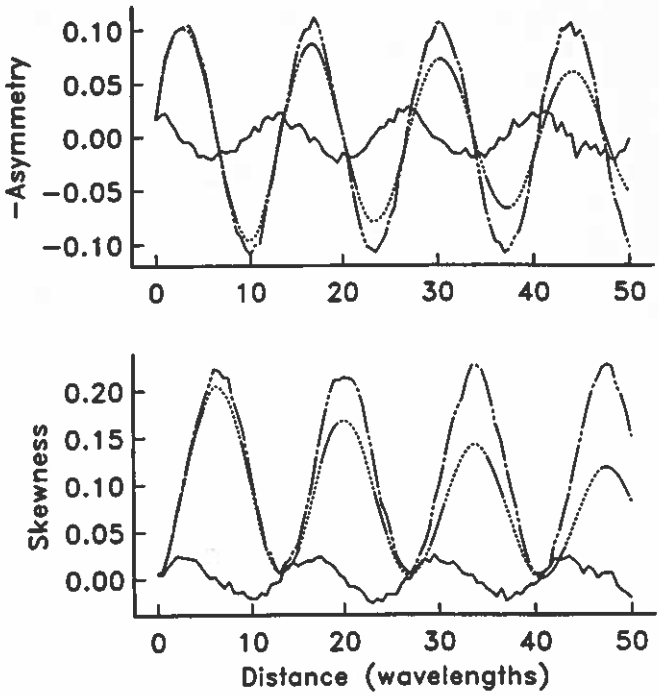

FIG. 2. Comparison of Evolution of Water-Surface Elevation Asymmetry and Skewness between Linear Inviscid (li), Nonlinear Inviscid (ni), and Nonlinear Viscous (nv) Boussinesq Models

tions that were initialized by either observed Fourier coefficients or by synthetic amplitudes and phases chosen from a Gaussian population having the desired frequency spectrum. In the present paper, however, the purely deterministic model is entirely appropriate. Averages across ensembles of initial conditions are not necessary because the laboratory data were generated by deterministic paddle motions at fixed frequencies.

Unless stated otherwise, the numerical simulations allowed 256 frequency modes, and had initial conditions consisting of a single sinusoid within a low-level background. Background energy levels were 1% that of the power spectral primary peak frequency, and the initial phases of the background waves were random with a uniform distribution. Energy transfers to several harmonics were allowed, with the maximum frequency ($\sim 6f_p$) included in the calculations corresponding to about $kh = 2.6$. Previous simulations have shown that the results are not sensitive to the precise high-frequency cutoff used in the integrations.

For the present nearly monochromatic initial conditions, discrete modal amplitudes at the primary and harmonic frequencies (f_p, $2f_p$, $3f_p$, . . .) will be examined. For the case of a fixed number of modes and essentially

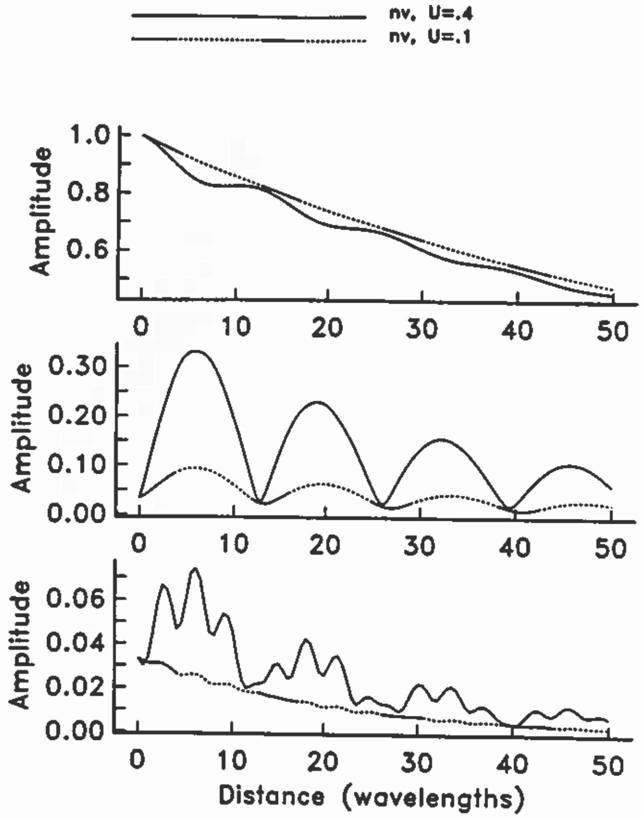

FIG. 3. Comparison of Evolution of Harmonic Amplitudes between Waves with Different Ursell Numbers

monochromatic initial conditions, the wave evolution is primarily a function of f_p, h, and the initial amplitude at f_p. The Ursell number U given by

$$U = \frac{\left(\frac{a}{h}\right)}{(kh)^2} \quad \text{(5)}$$

is a convenient nondimensional representation of initial nonlinearity. The wave number k in (5) corresponds to the power spectral peak frequency f_p, and the amplitude a is defined as twice the standard deviation of the water surface.

As shown by (2), both nonlinearity and dissipation can cause spatial changes in modal amplitudes and phases, which determine the sea-surface geometry (wave shape). Because the waves are weakly dispersive, their shapes change slowly as they propagate even in the absence of nonlinearity and viscosity. Laminar viscosity acts to increase the dispersive nature of the waves, while nonlinear-phase effects can have either sign, depending on the modal phases of the interacting waves. Just as significant wave height can

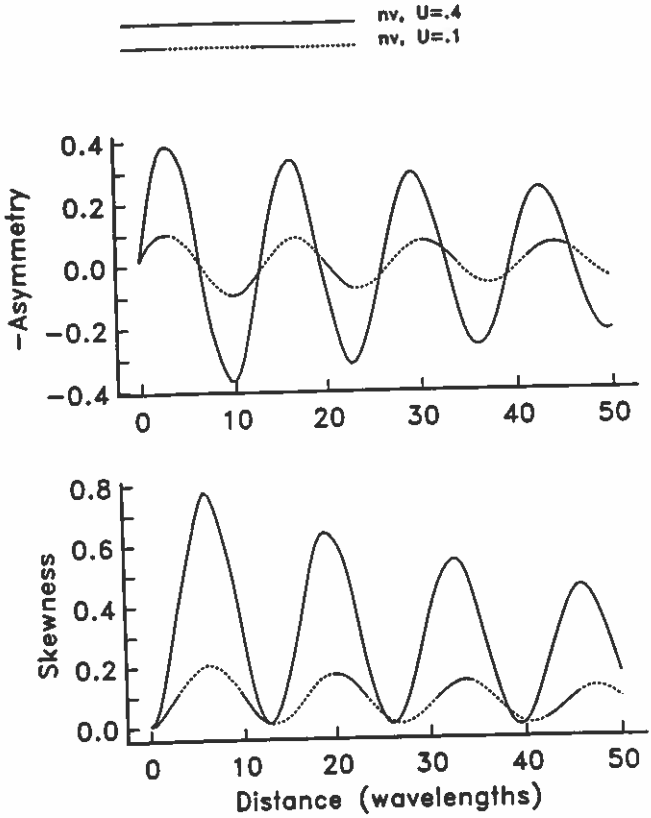

FIG. 4. Comparison of Evolution of Water-Surface Elevation Asymmetry and Skewness between Waves with Different Ursell Numbers

be used as an overall measure of wave amplitudes, the normalized third moments, skewness and asymmetry, are used as measures of nonsymmetric wave shapes and indicate asymmetry about horizontal and vertical axes, respectively (Elgar and Guza 1985). A pitched-forward wave (steep front face and gently sloping rear face) has positive asymmetry, while a Stokes wave (peaky crest and broad, flat trough) has positive skewness. Both skewness and asymmetry are zero for linear waves.

The effects of linear dispersion, nonlinearity, and viscosity on wave evolution are illustrated in Figs. 1 and 2. For these weakly nonlinear waves, $U = 0.1$ and $kh = 0.26$. In Fig. 1 (and all subsequent similar figures), the upper panel is the amplitude of the power spectral primary peak f_p, and the center and lower panels are the harmonic amplitudes at $2f_p$ and $3f_p$, respectively. The amplitudes have been normalized by the value of the primary amplitude at the initial conditions (distance = 0).

For inviscid linear waves on a flat bottom (solid line in Fig. 1) there is, of course, no amplitude evolution. Frequency dispersion between motions at f_p and the harmonics results in cycles in the normalized third moments (asymmetry and skewness, solid line in Fig. 2), with both asymmetry and

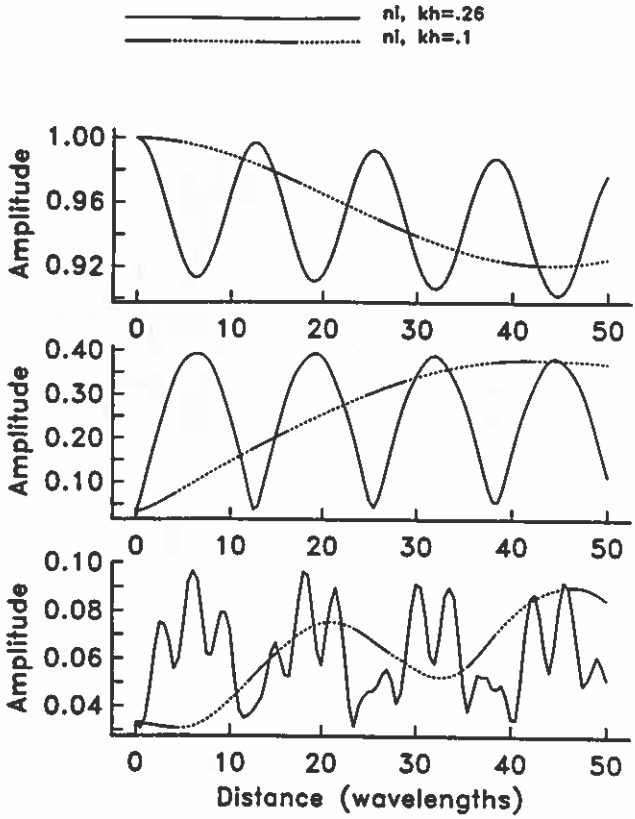

FIG. 5. Comparison of Evolution of Harmonic Amplitudes between Waves with Different Dispersiveness

skewness oscillating slightly about 0. It can be shown that the initial phase of the oscillations depends on the initial modal phases.

When nonlinear interactions are allowed (dashed lines in Figs. 1 and 2) energy is exchanged between the primary and its harmonics, leading to oscillations in modal amplitudes (Fig. 1). On the linear scales used in Fig. 1, the amplitude of the primary wave does not change appreciably, while that of the second harmonic periodically increases to more than 2.5 times its initial value (but never becomes significantly less than its initial value), while the third harmonic amplitude oscillates approximately about its initial value.

The most striking difference between the (inviscid) linear and nonlinear cases is in the evolution of third moments. The introduction of even weak nonlinearity significantly increases the amplitudes of the oscillations of third moments. Furthermore, the character of the oscillations changes fundamentally. In the linear case the initial derivatives of both asymmetry and skewness depend on the initial modal phases. That is, the asymmetry and skewness may initially increase or decrease. In the nonlinear case, with monochromatic initial conditions, asymmetry still oscillates about 0 (corresponding to wave shapes cycling from pitched forward to pitched back-

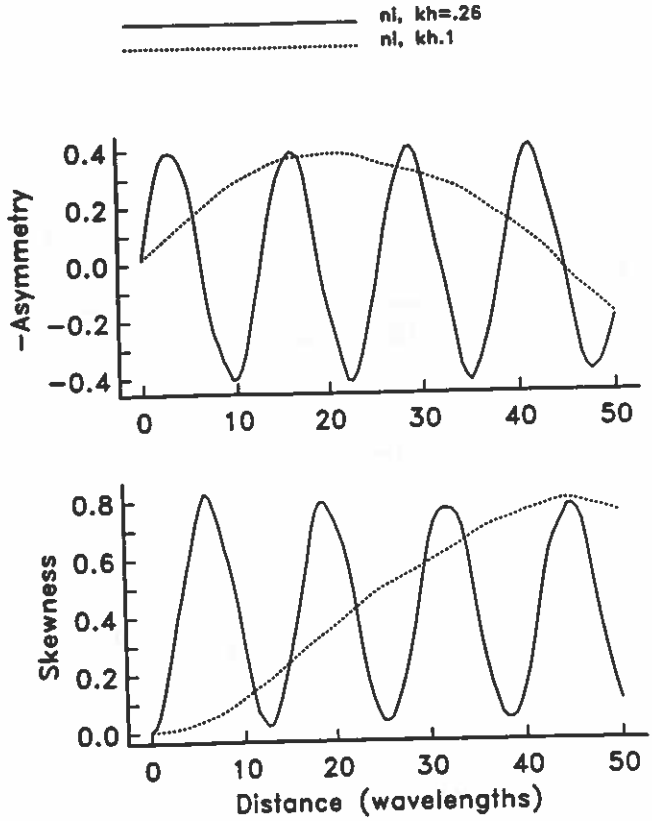

FIG. 6. Comparison of Evolution of Water-Surface Elevation Asymmetry and Skewnes between Waves with Different Dispersiveness

ward), but the initial derivative is always toward greater negative asymmetry (corresponding to increasingly pitched-forward shapes), independent of the initial modal phases (Elgar and Guza 1986). Nonlinear interactions force the phase of the (initially small) second harmonic to become locked to that of the primary, and the relative phase between the harmonics is primarily determined by the nonlinear term in (2*b*). Similarly, the skewness oscillations result from nonlinearly induced phase locking (rather than the initial phases), and skewness initially increases.

When both nonlinearity and viscosity are included, laminar viscosity (long dashes separated by dotted lines) reduces the energy levels at each frequency band as the waves propagate. Because the total energy of the system is monotonically decreasing, nonlinear interactions become progressively weaker (Fig. 1). The effect of viscosity on the normalized third moments (asymmetry and skewness) is less pronounced than on amplitudes (Fig. 2).

The fluctuations of harmonic amplitudes (Fig. 3) and third moments (Fig. 4) for viscous, moderately nonlinear waves ($U = 0.4$, solid line) have larger amplitudes than for weakly nonlinear waves ($U = 0.1$, long dashes separated by dotted lines). On the other hand, the wavelengths of the cycles of har-

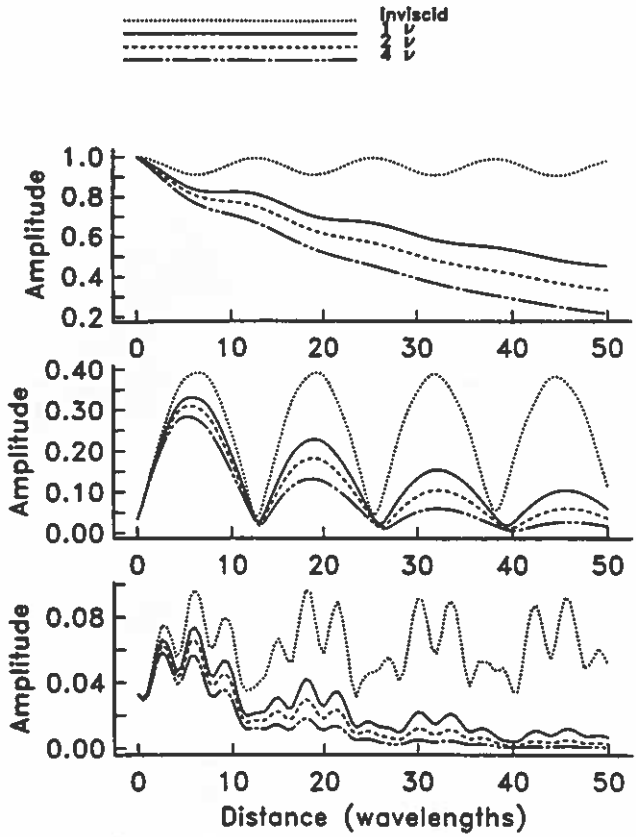

FIG. 7. Comparison of Evolution of Harmonic Amplitudes between Waves with Different Viscosity

monic amplitudes and third moments are similar in the moderately nonlinear and weakly nonlinear cases.

The effect of dispersion on the evolution of nonlinear, inviscid waves is shown in Figs. 5 and 6. More dispersive waves ($kh = 0.26$, solid line) have much more rapid oscillations in the evolution of harmonic amplitudes and third moments than do less dispersive waves ($kh = 0.1$, long dashes separated by dotted lines). However, at constant U($U = 0.4$ here) the sizes of the modulations are similar, with harmonic amplitudes (as a percentage of the primary amplitude) and third moments reaching almost equal minimum and maximum values. The results illustrated in Figs. 1–6 are predicted by a two-mode model (Mei and Ünlüata 1972) and appear to also hold in the present many-mode formulation.

The inclusion of viscosity for moderately nonlinear waves ($U = 0.4$, $kh = 0.26$) results in decreasing harmonic amplitudes, and the evolution is qualitatively similar for viscosities varying by a factor of 4, as shown in Fig. 7 [the dotted line is the nonlinear inviscid model, the solid line is a nominal viscosity for water ($\nu = 0.01$ cm^2/s), equal sized dashes are 2ν, and long dashes separated by 1 and 2 short dashes are 4ν]. In all cases shown, non-

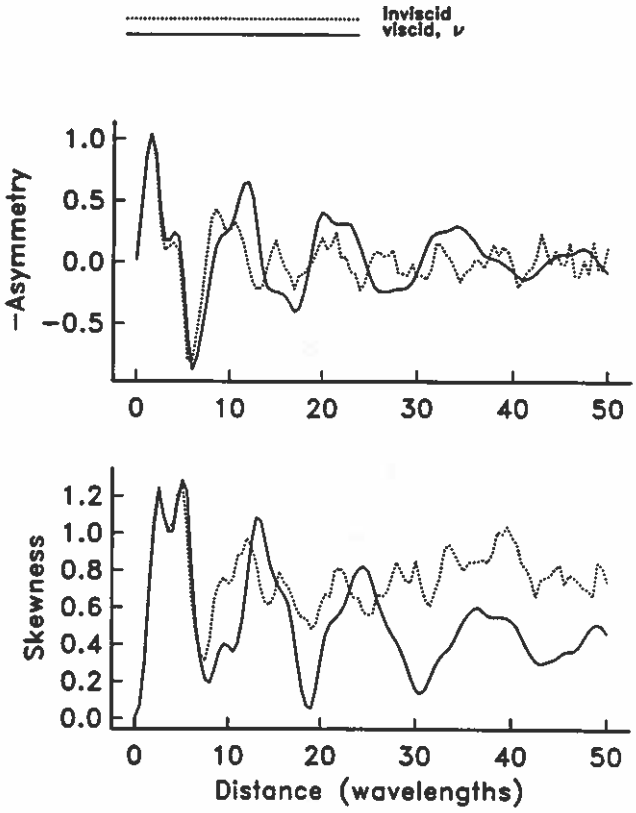

FIG. 8. Comparison of Evolution of Water-Surface Elevation Asymmetry and Skewness between Inviscid and Viscous Waves

linearity causes spatially periodic modal energy transfers, although the relative maximum amplitudes of the harmonics decrease with increasing frequency at all propagation distances. While viscosity decreases all modal amplitudes, it does not qualitatively change the nature of the nonlinear cross-spectral energy transfers for this moderately nonlinear system.

Dissipation does, however, qualitatively modify the spatial evolution of more nonlinear systems, as shown in Fig. 8 for $U = 1.6$ and $kh = 0.26$. Whereas several recurrence cycles (defined here as near returns to initial amplitudes and third moments) are evident for inviscid waves with $U = 0.4$ (Figs. 5 and 6), the inviscid model for $U = 1.6$ (dotted line in Fig. 8) predicts a relatively rapid damping of the cycles in the evolution of third moments (see also Elgar et al. 1990a). The addition of viscosity (solid line) prolongs the cycling of third moments, and although the maximum and minimum values of asymmetry and skewness decrease as the waves evolve, the cycles persist for at least 50 wavelengths.

Laboratory Experiments

In all the nonlinear, viscous cases described earlier, the Boussinesq model predicts significant energy exchange between motions with frequency f_p (the

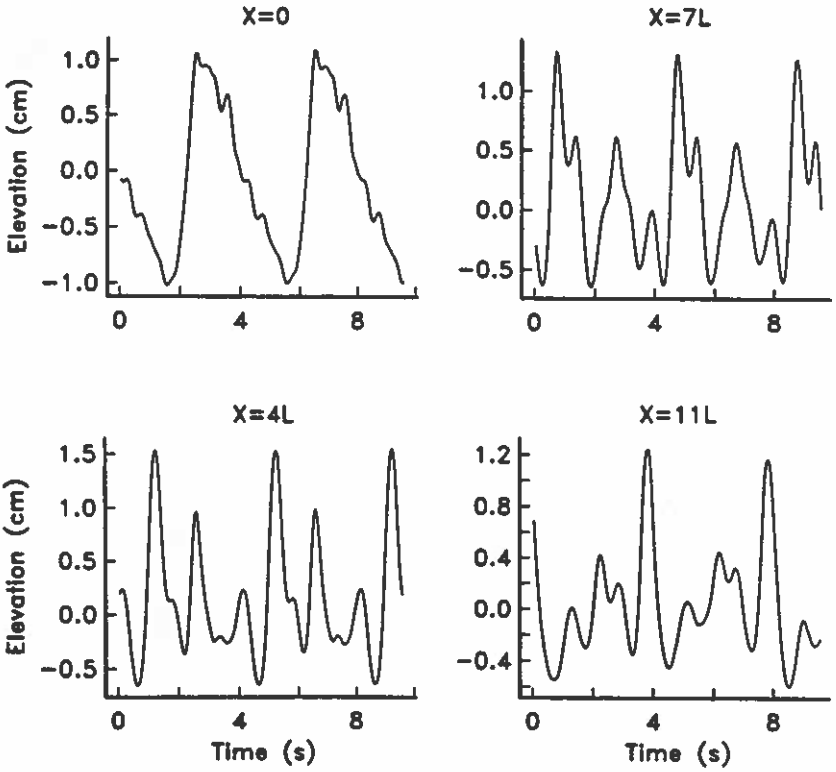

FIG. 9. Time Series of Water Elevation Observed in Laboratory

initial power spectral peak) and motions at $2f_p$, $3f_p$, and so forth. When the harmonic amplitudes are comparable to the primary amplitude, multiple crests appear (frequency doubling and frequency trebling). In addition, the Boussinesq model predicts rather extreme changes in the shapes of the waves, with profiles that steepen and pitch forward and then unsteepen and pitch backward, as indicated by the cycles of third moments.

To test these predictions, experiments were conducted in a 1.8 m wide, 10.5 cm deep, wave flume (Hughes and Fowler 1990) at the U.S. Army Corps of Engineers Waterways Experiment Station in Vicksburg, Miss. The distance from the piston-type wavemaker, driven at a single frequency, to the toe of a 1/40 sand beach was 46 m. Wave elevations were measured over the constant depth portion of the flume with 4 capacitance gauges located 4, 19, 31, and 46 m from the wavemaker. Waves with peak frequencies in the range $0.25 < f_p < 0.4$ Hz and amplitudes between approximately 0.25 and 5 cm were generated. Thus, $0.2 < U < 8$ and $0.16 < kh < 0.26$. The water surface elevation at each gauge for the case of $f_p = 0.25$, $U \sim 2$, and $kh = 0.26$ is shown is Fig. 9. At the gauge closest to the wavemaker ($X = 0$ in Fig. 9), the water-surface oscillations have a 4 sec period, although the profile is not sinusoidal. At $X = 4L$ and $X = 7L$, where L is the wavelength corresponding to f_p ($L \sim 3.9$ m in this case), the waves have frequency trebled, with 3 distinct crests over each 4 sec period

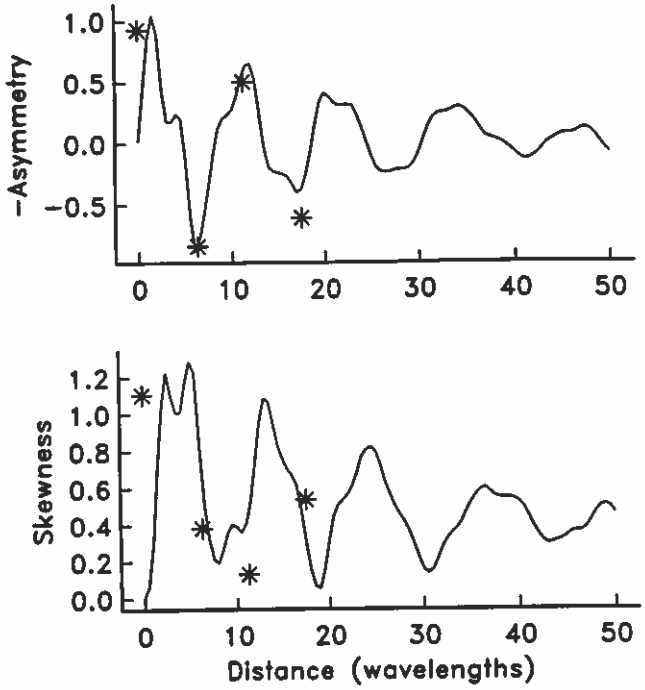

FIG. 10. Comparison of Third Moments Observed in Laboratory with Predictions of Nonlinear Viscous Boussinesq Model for Initial Wave Field Consisting of Sinusoid in Low-Level Noise

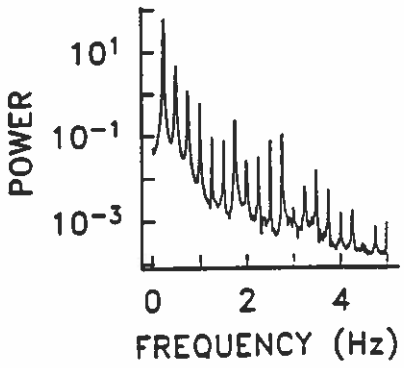

FIG. 11. Power Spectrum of Water Elevation (Fig. 9) Observed at $X = 0$

(frequency doubling was observed in other cases). The power spectrum (not shown) at $X = 11L$ shows spectral levels at $3f_p$ and $4f_p$ as high as those at f_p.

Not only was frequency doubling, trebling, and possibly quadrupling observed, but the laboratory waves developed steep, pitched-forward profiles,

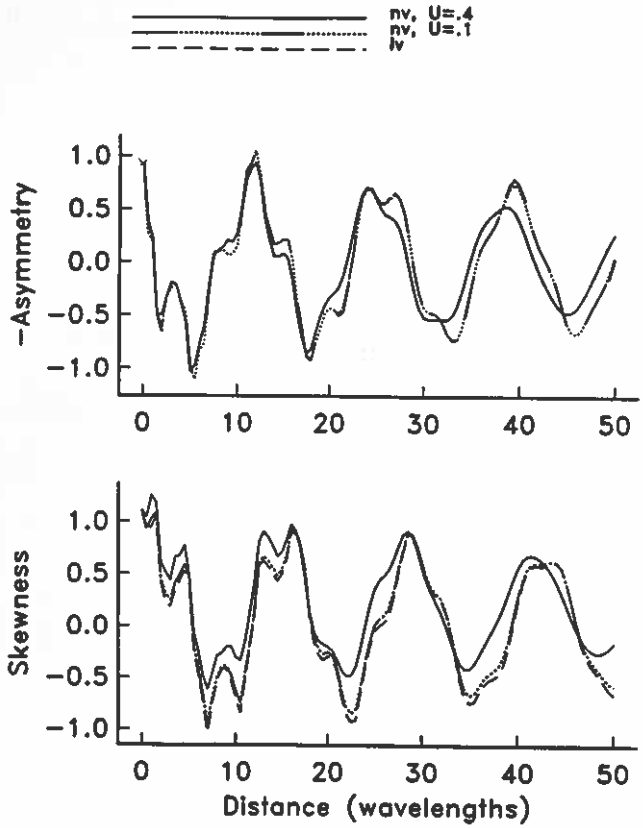

FIG. 12. Comparison of Water-Surface Elevation Asymmetry and Skewness between Linear Waves and Waves with Different Ursell Number

and then unsteepened and pitched backward, as shown by the symbols in Fig. 10. As shown by the solid line in Fig. 10, the observed evolution of asymmetry and skewness is qualitatively similar to nonlinear, viscous Boussinesq model predictions for the case of an initial sinusoid (f_p = 0.25 Hz) in a low level background with U = 1.6 and kh = 0.26. However, the comparison is only approximate because the initial conditions differed between the laboratory and model runs.

To compare laboratory data quantitatively to model predictions, the model must be initialized using the observations at the first gauge. The observed spectrum (units are arbitrary) at X = 0 (Fig. 11) shows that the laboratory waves for X = 0 do not consist of a single sinusoid within a low-level background. The substantial harmonic peaks in the spectrum are much larger than predicted by nonlinear wavemaker theory (Madsen 1971). If the viscous Boussinesq model is initialized with a wave field similar to that shown in Fig. 11, linear dispersive effects dominate the evolution of the third moments, as shown in Fig. 12 for kh = 0.26 and U = 0.1 (dashes separated by dotted lines) and U = 0.4 (solid line). The dashed line is linear, viscous Boussinesq theory. Linear dispersion results in phase shifts

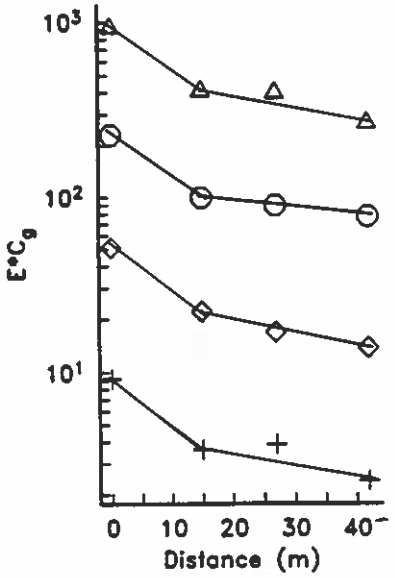

FIG. 13. Observed Dissipation (Decreasing Energy Flux) for Four Initial Wave Heights

between the Fourier components similar to that shown in Fig. 2. However, in the case of many large, phase-coupled harmonics in the initial spectrum (Fig. 12), the third moments initially have large values of asymmetry and skewness, and the linear and nonlinear evolution of third moments are very similar. Thus, although the nonlinear Boussinesq model can be compared to the observations, in this case it would be difficult to separate nonlinear from linear effects.

Inviscid linear waves on a flat bottom have no amplitude evolution, and linear, but viscous waves have exponentially decaying amplitudes. On the other hand, nonlinear waves have more complicated evolution of harmonic amplitudes, and thus, in principle, model-data comparisons of harmonic amplitudes could be used to distinguish linear from nonlinear evolution in cases where third moments evolve similarly (e.g. Fig. 12). However, the dissipation observed in the flume was not laminar, and could not be accounted for with a simple increase in the effective value of viscosity nor with a quadratic parameterization. As shown in Fig. 13, more dissipation occurred between the first two gauges then between gauge 2 and gauge 4. If the dissipation was laminar, all four points would lie on a straight line and the slope of the line would be the same for all wave heights. If the dissipation was quadratic, there would be relatively more dissipation for large waves than for small waves. As shown in Fig. 13, between gauges 2 and 4 the relative rate of change of energy flux (EC_g, where E is the wave energy and C_g is the group velocity corresponding to f_p) with propagation distance is more-or-less constant for wave fields varying by two orders of magnitude in initial energy. However, the rate of change of EC_g with distance between gauges 1 and 2 differs substantially from that between gauges 2 and 4. The reasons for this apparently nonlaminar dissipation are unknown. It may have resulted from inhomogeneities in the wave flume, or

from a more fundamental difficulty related to estimating the damping of these nonlinear, nonbreaking, waves. Regardless, nonlaminar dissipation is not incorporated in the Boussinesq model used here, and no further model-data comparisons were made.

Conclusions

The roles of frequency dispersion, nonlinearity, and laminar viscosity in the evolution of long waves in constant depth were investigated with numerical solutions of the discretized and truncated many-mode Boussinesq equations. The parameters of the simulated waves were suitable for observing wave evolution over many wavelengths in a moderately long laboratory flume. As expected, viscosity reduces the effect of nonlinearity by decreasing the wave energy. In particular, the predicted broadening of an initially narrow wave spectrum as a consequence of moderate nonlinearity (with no viscosity) is delayed.

Preliminary laboratory results show some qualitative similarities to the numerical simulations. As predicted, wave crests were not conserved, and frequency doubling and trebling were pronounced. The initial evolution of the wave shape to a pitched-forward front face and peaky crests (usually a precursor to wave breaking on a sloping beach) was followed by development of a steep rear face and a nearly symmetric crest/trough profile.

However, these laboratory experiments were not suitable for detailed model-data comparsions. First, although the piston wavemaker was programmed to oscillate in simple harmonic motion, it generated waves with significant amplitudes at the harmonics of the primary motion (these harmonics were larger than predicted by nonlinear wavemaker theory). Numerical simulations show that these initially large harmonics obscure some of the effects of nonlinearity by amplifying the importance of linear frequency dispersion. Although the initial conditions were not ideal, in principle the large harmonic amplitudes could have been accounted for in the numerical model. On the other hand, the dissipation observed in the flume was not laminar, and could not be accounted for either with a simple increase in the effective value of viscosity, or with a quadratic parameterization. More carefully controlled experiments are required to provide observations over long propagation distances for quantitative comparisons to Boussinesq model predictions.

Acknowledgments

This research was supported by the Physical Oceanography Program of the National Science Foundation (NSF). Portions of the research were performed at the Jet Propulsion Laboratory, California Institute of Technology, under contract to NASA. The computations were performed at the San Diego Supercomputer Center (supported by NSF). J. Fowler and D. Daily helped with the laboratory experiments.

Appendix. References

Abbott, M. B., Peterson, H. M., and Skovgard, O. (1978). "On the numerical modelling of short waves in shallow water." *J. Hydr. Res.*, 16, 173–203.

Buhr-Hansen, J., and Svendsen, I. A. (1974). "Laboratory generation of waves of constant form." *Proc., 14th Int. Conf. on Coast. Engrg.*, ASCE, 321–329.

Elgar, S., and Guza, R. T. (1985). "Observations of bispectra of shoaling surface gravity waves." *J. Fluid Mech.*, 161, 425–448.

Elgar, S., and Guza, R. T. (1986). "Nonlinear model predictions of bispectra of shoaling surface gravity waves." *J. Fluid Mech.*, 167, 1–18.
Elgar, S., Freilich, M. H., and Guza, R. T. (1990a). "Recurrence in truncated Boussinesq models for nonlinear waves in shallow water." *J. Geophysical Res.*, 95, 11547–11556.
Elgar, S., Freilich, M. H., and Guza, R. T. (1990b). "Model-data comparisons of moments of nonbreaking shoaling surface gravity waves." *J. Geophysical Res.*, 95, 16055–16063.
Freilich, M. H., and Guza, R. T. (1984). "Nonlinear effects on shoaling surface gravity waves." *Philosophical Transactions of the Royal Society of London*, London, England, A311, 1–41.
Hughes, S. A., and Fowler, J. E. (1990). "Midscale physical model validation for scour at coastal structures." *Tech. Rep. CERC-90-8*, U.S. Army Corps of Engineers, Vicksburg, Miss.
Liu, P., Yoon, S., and Kirby, J. (1985). "Nonlinear refraction-diffraction of waves in shallow water." *J. Fluid Mech.*, 153, 184–201.
Madsen, O. S. (1971). "On the generation of long waves." *J. Geophysical Res.*, 36, 8672–8683.
Madsen, P., and Warren, I. (1984). "Performance of a numerical short-wave model." *Coast. Engrg.*, 8, 73–79.
Mei, C. C., and Ünlüata, U. (1972). "Harmonic generation in shallow water waves." *Waves on beaches*, R. E. Meyer, ed., Academic Press, New York, N.Y., 181–202.
Peregrine, D. H. (1967). "Long waves on a beach." *J. Fluid Mech.*, 27, 815–827.
Peregrine, D. H. (1972). "Equations for water waves and the approximations behind them." *Waves on beaches*, R. E. Meyer, ed., Academic Press, New York, N.Y., 95–122.
Rygg, O. (1988). "Nonlinear refraction-diffraction of surface waves in intermediate and shallow water." *Coast. Engrg.*, 12, 191–211.
Van Dorn, W. G. (1966). "Boundary dissipation of oscillatory waves." *J. Fluid Mech.*, 24, 769–779.
Vengayil, P., and Kirby, J. T. (1986). "Shoaling and reflection of nonlinear shallow water waves." *Rep. UFICOEL-TR/062*, Coastal and Ocean Engineering Dept., Univ. of Florida, Gainesville, Fla.